ACS Catalysis

Research Article

pubs.acs.org/acscatalysis

Heterogeneous Catalysis on Atomically Dispersed Supported Metals: CO_2 Reduction on Multifunctional Pd Catalysts

Ja Hun Kwak,*[,†,§] Libor Kovarik,[‡] and János Szanyi*[,†]

[†]Institute for Integrated Catalysis and [‡]Environmental Molecular Sciences Laboratory, Pacific Northwest National Laboratory, Richland, Washington 99352, United States

ABSTRACT: Because of their heterogeneous nature, supported metal catalysts always contain metal centers in a rather broad dispersion range, and the presence of even atomically dispersed metals has been reported on oxide supports. The role of the atomically dispersed metal centers in the overall catalytic performances of these supported metal catalysts, however, has not been addressed to date. In this study, temperature programmed reaction and scanning transmission electron microscopy experiments were applied to show the fundamentally different reactivity patterns exhibited by Pd metal in atomically dispersed and traditional 3D clusters in the demanding reaction of CO_2 reduction. The requirement for two different catalyst functionalities in the reduction of CO_2 with hydrogen on Pd/Al_2O_3 and Pd/MWCNT catalysts was also substantiated. The results obtained clearly show that the oxide support material, even when it is considered inert like Al_2O_3, can function as a critical, active component of complex catalyst systems.

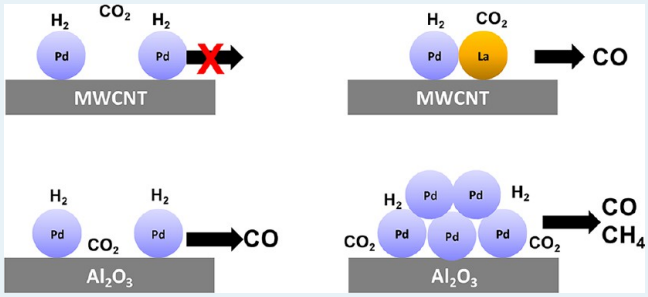

KEYWORDS: *CO_2 reduction, product selectivity, bifunctionality, atomic metal dispersion, supported Pd catalysts*

INTRODUCTION

Oxide-supported metals represent the most common heterogeneous catalysts used in a number of high volume industrial processes. In most of these systems the active metal component is present as three-dimensional (3D) clusters (ranging from a few nm to tens of nm). Recently, in particular since the discovery of very high catalytic activity of fine Au nanoparticles on oxide supports, significant efforts have been devoted to investigate and understand the catalytic chemistry over very small, nm-sized metal clusters.[1,2] For a number of catalytic systems maximum activity was observed when the metal cluster size decreased to 2−3 nm, but the activity was shown to drop below ∼2 nm.[2] Recent studies on size-selected supported metal cluster model catalysts indicate that very different catalytic activities and selectivities can be expected on metal centers present in sizes of subnanometer scale.[3] Ultimately the utilization of single metal atoms in heterogeneous catalysis would be highly desirable to maximize the efficiency of each active center. Because of the heterogeneous nature of practical catalysts the preparation and subsequent utilization of single metal atoms on oxide supports have not been widely demonstrated. The oxidation of CO on single metal atoms supported on iron oxide has been shown recently to proceed with very high atom efficiency.[4] In contrast, most of the highly active homogeneous catalysts contain mono-, or diatomic metal centers as active sites, and exhibit very high selectivities for specific reactions. Attempts to "heterogenize" homogeneous catalysts by anchoring them to solid supports (mostly oxides) were mostly unsuccessful, due primarily to the strong interaction between the active homogeneous catalyst and the support that was detrimental to the activity of these systems. Therefore, there is very little knowledge about the catalytic properties of metal centers in atomic dispersion on oxide supports. As the metal particle size decreases below 1 nm and the dispersion approaches atomic, we can expect large influence of the support on the catalytic properties of the active phase, and increasing influence of the active metal/support interface on the overall catalytic activity of a metal-oxide system.

The conversion of CO_2 to high energy density organic molecules (methanol or methane) has been proposed over both homogeneous and heterogeneous catalysts containing Cu, Ni, and Pd.[5−7] Considerable work has been aimed at designing and synthesizing heterogeneous CO_2 reduction catalysts. The activity and selectivity of these catalysts have been shown to be very sensitive to the cluster size and the shape of the metal particles dispersed on the support, as well as to the interaction between the active metals and oxide supports.[8,9] However, these features of oxide-supported metal catalysts remain, to a great extent, uncontrollable because of the nature of synthetic protocols, and sintering of metal clusters during the activation process. The heterogeneous catalytic conversion of CO_2 is currently not feasible because of the demanding reaction conditions (e.g., high catalyst bed temperature) originating from the chemical inertness of CO_2. Therefore, understanding

Received: February 21, 2013
Revised: July 8, 2013
Published: July 17, 2013

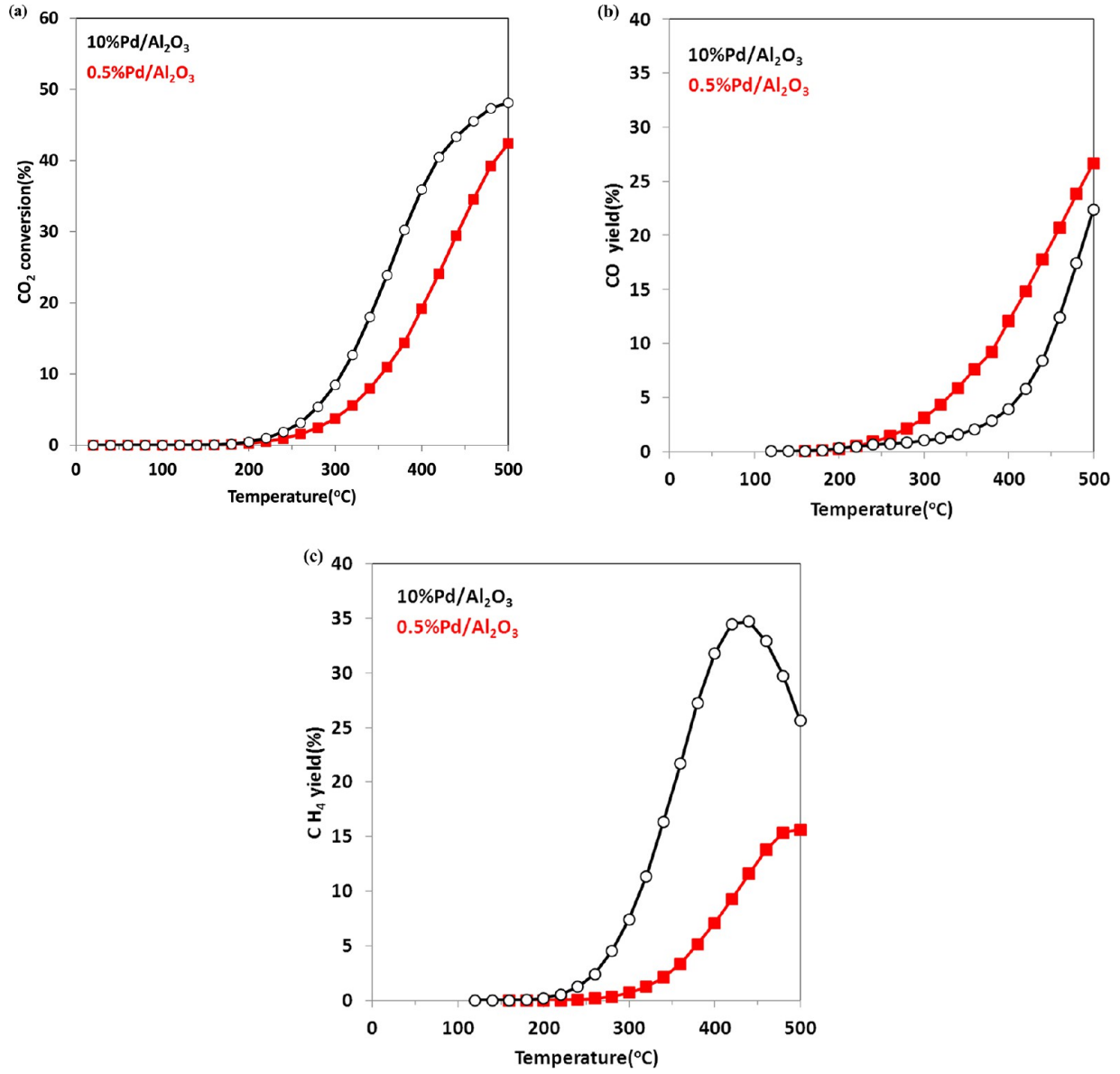

Figure 1. CO_2 conversion (a), and CO (b)/CH_4 (c) yield profiles during CO_2 reduction reaction on 10% (black) and 0.5% (red) Pd/Al_2O_3. (50 mg of catalysts with 5% CO_2 +15% H_2 in He (total flow rate = 1 mL/s), temperature programmed reaction with heating rate = 5 °C/min).

the elementary reaction steps of catalytic CO_2 reduction is critical to design economically viable catalytic systems. Despite the ongoing research efforts, the role of supports and the control of CO/CH_4 selectivity in the reduction of CO_2 with H_2 have not been well established, in particular not on subnanometer-sized supported metal atoms/clusters.[10−12] In this study we compare the catalytic properties of atomically dispersed Pd particles to those of metal clusters in the highly demanding reaction of CO_2 reduction. Atomically dispersed Pd supported on an oxide (e.g., Al_2O_3) displays high activity in the reduction of CO_2, while Pd in the same dispersion is completely inactive for CO_2 reduction when it is supported on inert multiwall carbon nanotubes (MWCNT). The addition of an oxide component (e.g., La_2O_3) to the inactive Pd/MWCNT system results in the formation of a highly active CO_2 reduction catalyst. These results underline the importance of multifunctionality in a working catalyst for the reduction of CO_2.

EXPERIMENTAL SECTION

Al_2O_3-supported, 0.5% and 10 wt % Pd catalysts were prepared on a commercial γ-Al_2O_3 powder (Condea, BET surface area = 200 m^2/g) by the incipient wetness method using $Pd(NH_3)_4(NO_3)_2$ as the precursor.

CO_2 reduction activity measurements were conducted by temperature programmed reaction methods in a packed bed reactor using 50 mg of catalyst powder samples (quartz reactor O.D. = 1/2″). The catalysts were activated prior to catalytic measurements by calcination at 500 °C for 2 h under 6.7% O_2/He (flow rate = 60 mL/min) and followed by reduction at 500 °C for 30 min under 15% H_2/He (flow rate = 60 mL/min). The activity was measured using a feed gas mixture containing 5% CO_2 and 15% H_2 in He (total flow rate = 60 mL/min and H_2/CO_2 = 3). The concentrations of all reactant and product species were measured by a gas chromatograph (HP 7820), with separation using a capillary column (Supelco, Carboxene-1006 PLOT, 30m × 0.53 mm I.D.) and a thermal conductivity detector.

dx.doi.org/10.1021/cs4001392 | ACS Catal. 2013, 3, 2094−2100

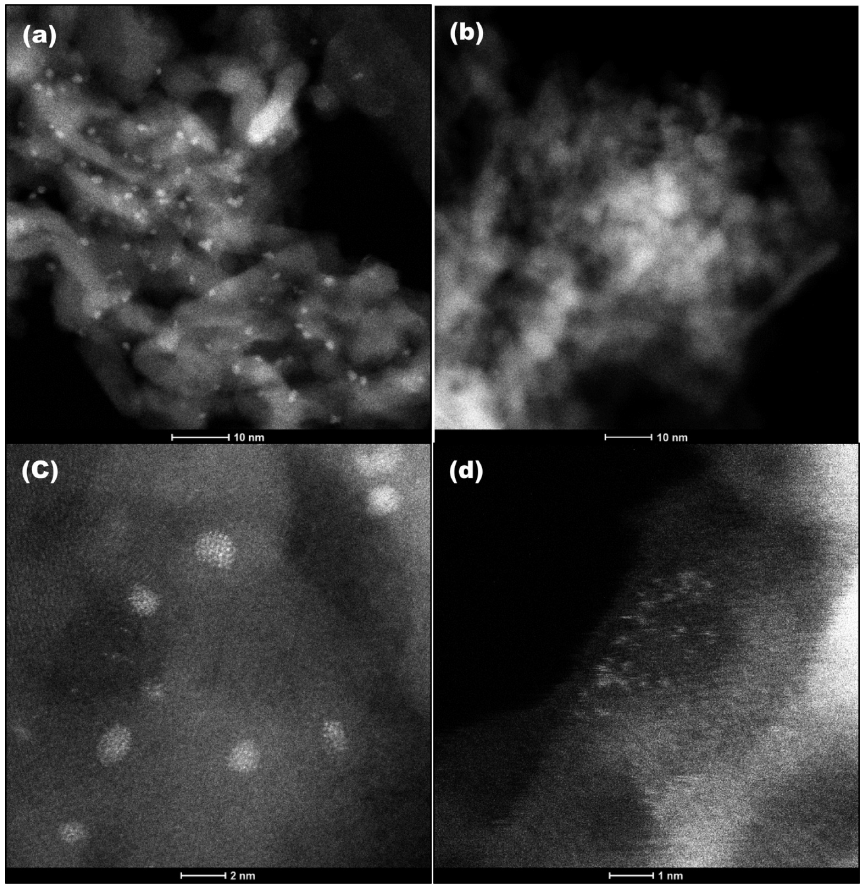

Figure 2. STEM images on 10% (a,c) and 0.5% Pd/Al_2O_3 (b,d). (STEM images were obtained from the "fresh" catalysts after calcination and reduction (both at 500 °C), but without reaction tests.).

1% Pd and 1% Pd+2.3% La_2O_3 supported on multiwalled carbon nanotube (MWCNT) were prepared by wet impregnation of $Pd(NH_3)_4(NO_3)_2$ and La_2O_3 dissolved in 10% HNO_3 on a commercial MWCNT (Cheap Tube Inc., O.D. = 20−30 nm, BET surface area = 110m^2/g). The as-purchased MWCNT were treated by concentrated HNO_3 under reflux condition for 16 h for surface functionalization.[19−21] MWCNTs were washed excessively using distilled water until neutral pH was achieved, then dried in a 100 °C oven overnight. The 1% Pd and 1% Pd +2.3% La_2O_3/MWCNT were activated prior to reaction tests by reduction at 300 °C for 30 min under 15% H_2/He (flow rate = 60 mL/min) and subsequent purging under flowing He (flow rate = 60 mL/min) at 300 °C for 2 h.

High-resolution TEM imaging was performed with a FEI Titan 80-300 microscope operated at 300 kV. The instrument is equipped with a CEOS GmbH double-hexapole aberration corrector for the probe-forming lens, which allows imaging with 0.1 nm resolution in scanning transmission electron microscopy (STEM) mode. The images were acquired in high angle annular dark field (HAADF) with an inner collection angle of 52 mrad. The sample preparation for the TEM measurements involved mounting of the powder samples on lacey carbon TEM grids, and immediate loading into the TEM airlock to minimize extended exposure to atmospheric O_2.

RESULTS AND DISCUSSION

Temperature programmed reaction method was used to evaluate the CO_2 reduction activities and CO/CH_4 selectivities of 0.5 and 10 wt % Pd/Al_2O_3 catalysts after calcinations in O_2 flow followed by reduction with H_2, both at 500 °C. Figure 1 displays CO_2 conversion (panel a) and yields of CO (panel b) and CH_4 (panel c) obtained in the temperature programmed CO_2 reduction experiments on 10% and 0.5% Pd/Al_2O_3 samples. On the 10% Pd/Al_2O_3 sample, the onset temperature of CO_2 reduction is ∼200 °C and the CO_2 conversion increases monotonically with temperature, then starts to level off above 400 °C. On the 0.5% Pd/Al_2O_3 sample CO_2 reduction starts at a similar temperature, but the overall CO_2 conversion remains significantly lower than on the 10% Pd-containing catalyst because of the much lower Pd loading. However, at any given reaction temperature the CO yield on the 0.5% Pd/Al_2O_3 sample is much higher than that on the 10% Pd/Al_2O_3. The difference in methane yields over these two catalysts, however, is even more significant. On the 10% Pd/Al_2O_3 catalyst much higher methane yield is observed than over the 0.5% Pd/Al_2O_3 sample, and the maximum CH_4 yield at ∼400 °C coincides with the leveling off of the CO_2 conversion. Above 400 °C, the CH_4 yield decreases with increasing reaction temperature, which is related to the reforming reaction between the initially produced CH_4 and H_2O and/or dry reforming between CH_4 and CO_2.[15−20] These reforming reactions are responsible for the increased slope of the CO yield profile at temperatures above 400 °C on the 10% Pd/Al_2O_3 sample. The reduction of CO_2 to CH_4 is slower on the 0.5% Pd/Al_2O_3 catalyst than over the 10% Pd/Al_2O_3 sample. This could be due to the much lower amount of Pd, thus the lower number of catalytic sites on the 0.5% Pd/Al_2O_3 sample. However, the higher CO yield observed on the 0.5% Pd/Al_2O_3 sample suggests that this may not be the origin

dx.doi.org/10.1021/cs4001392 | ACS Catal. 2013, 3, 2094−2100

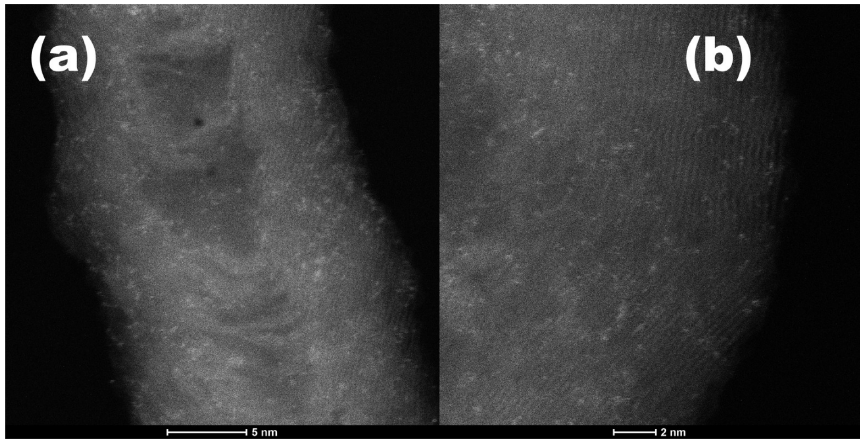

Figure 3. STEM images of 1% Pd/MWCNT (a) and 1% Pd+2.3% La_2O_3/MWCNT (b). (STEM images were taken after catalyst activation prior to catalytic tests.).

of the vastly different catalytic performance of these two Pd/Al_2O_3 catalysts in the reduction of CO_2. One possible explanation for the observed reactivity difference between these two catalysts is the dramatically different Pd particle size at the two Pd loadings studied here (0.5 vs 10%). The very different particle size, in turn, may bring about fundamental changes in the reaction mechanism over these two catalysts. Recently, we have demonstrated that the NH_3 conversion pathway on Cu/Al_2O_3 catalysts in NH_3 selective catalytic reduction (SCR) varied greatly with Cu cluster size.[14] NH_3 reacted selectively with NO to produce N_2 on monomeric CuO centers on alumina, while NO_x was produced on CuO clusters as NH_3 reacted with O_2. To visualize the Pd particles present in vastly different sizes over these two alumina-supported catalysts, STEM images were collected (selected images are shown in Figure 2) from the fresh, activated (oxidation and subsequent reduction) samples. STEM images of panels a and c in Figure 2 show the presence of nanosized (average particle size of ∼2 nm) Pd clusters in the 10% Pd/Al_2O_3 sample. On the other hand, no evidence for the presence of Pd clusters in the 0.5% Pd/Al_2O_3 sample can be seen in the low magnification image (Figure 2b). However, in the high magnification image of the 0.5% Pd/Al_2O_3 sample almost complete atomic dispersion of the Pd phase can be observed. Therefore, the STEM images presented here clearly substantiate the dramatic change in Pd cluster size as a result of Pd loading. Mostly atomically dispersed Pd is present at 0.5% metal loading, while nanosized Pd clusters are prevalent in the 10% sample. (STEM images obtained from samples after their use in the CO_2 reduction reaction revealed the formation of metal clusters in the 0.5% Pd-loaded samples, and the growth of particles in the 10% Pd-containing catalyst. Ongoing environmental TEM measurements are aimed at understanding the particle growth under reaction conditions as a function of Pd loading.) The next question we need to seek to answer is whether the interaction between Pd and the alumina support influences the reaction mechanism of CO_2 reduction, either by modifying the active metal phase or by creating interfacial sites that might be important in the activation and/or reduction of CO_2.

To elucidate the influence of the interaction between the oxide support and the active metal phase on the reaction mechanism of CO_2 reduction, we examined the performances of Pd particles supported on an inert material, namely, on functionalized multiwalled carbon nanotubes (MWCNT). This was done to eliminate, or minimize the effect of the support material on the catalytic behavior of the metal particles. The interaction of the metal and the alumina support has been known to be strong in Pt/Al_2O_3 systems, and was proven to be very important in the stabilization of high metal dispersion even at elevated temperatures.[13,18] The influence of this strong interaction between the active metal and the support on the catalytic properties of the metal/oxide systems, however, has not been studied in detail on alumina-supported metal catalysts. Besides the effect of the support material on the metal particles, the support itself might play an important role in the catalytic cycle as it may interact with the reactant(s), stabilize intermediates or reaction products, or create special interfacial sites where reactions can proceed. Modifying the SiO_2 support with MgO in a supported Pd catalyst Park and McFarland[12] observed a dramatic change in the catalyst selectivity in the reduction of CO_2 with H_2. On Pd/SiO_2 the almost exclusive formation of CO was observed, while on the MgO-modified catalyst CH_4 formed with high selectivity. The MgO/SiO_2 system showed no measurable activity in the reduction of CO_2. They rationalized their results by suggesting a bifunctional mechanism for the reduction of CO_2 on the Pd-MgO/SiO_2 catalyst. In their proposed mechanism CO_2 first strongly adsorbs onto MgO, while Pd dissociates H_2 to produce atomic hydrogen. The thus formed hydrogen atoms then can spill over to the nearby MgO-adsorbed CO_2, initiating its stepwise reduction to atomic C and its subsequent hydrogenation to CH_4. Since CO_2 can strongly interact with our Pd/Al_2O_3 catalysts to produce alumina-bound carbonates/bicarbonates, we chose an inert support (MWCNT) to eliminate the contribution of the support. We also prepared a Pd/MWCNT catalyst that was doped with La_2O_3 to create metal/oxide interfacial sites, and investigated their possible roles in the activation and reduction of CO_2.

Functionalized MWCNTs were prepared by the well-established acid treatment of the nanotubes.[19−21] The thus formed oxidized nanotube walls provide anchoring sites for the Pd particles. To this end we prepared two samples by a simple incipient wetness impregnation method: 1% Pd/MWCNT and (1% Pd+2.3% La_2O_3)/MWCNT. Representative STEM images collected after activation of these samples at 300 °C clearly demonstrate the presence of atomically dispersed Pd on the MWCNT, as shown in Figure 3a for the 1% Pd/MWCNT sample. Although, it is not trivial to distinguish between Pd and

dx.doi.org/10.1021/cs4001392 | ACS Catal. 2013, 3, 2094−2100

La atoms because of the low contrast difference, it is clear that the dispersion level in the Pd+La_2O_3/MWCNT sample (see Figure 3 b) is very similar to that observed for the 1% Pd/MWCNT.

The CO_2 conversion and CO/CH_4 selectivity results from the MWCNT-supported 1% Pd and 1% Pd+2.3% La_2O_3 samples, obtained under the same CO_2 reduction reaction conditions as those shown in Figure 1, are displayed in panels a and b of Figure 4, respectively. Under these temperature

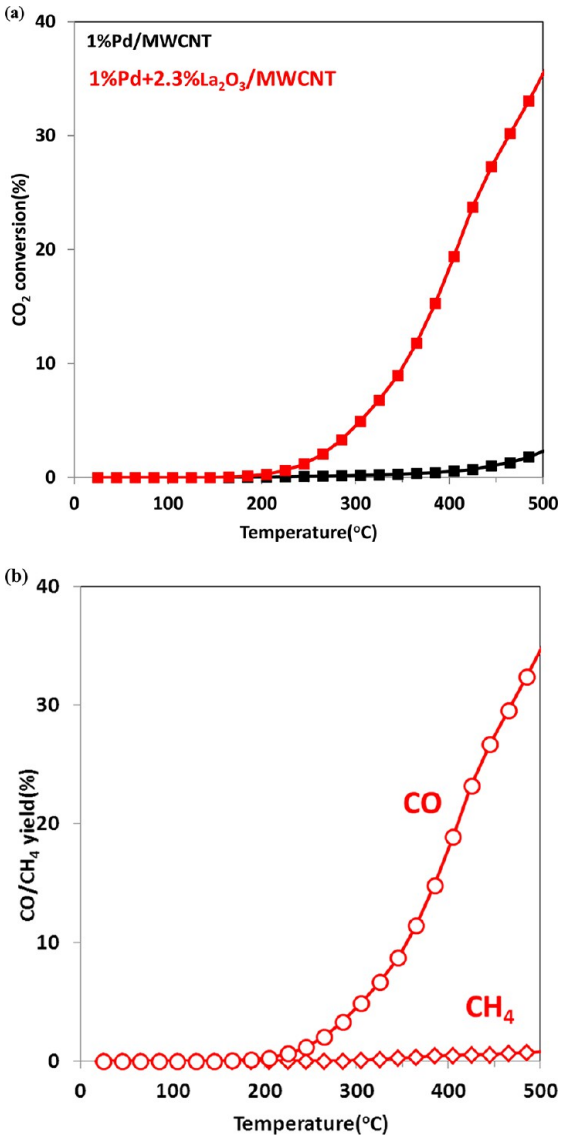

Figure 4. CO_2 conversion (a) on 1% Pd/MWCNT (black) and 1% Pd +2.3% La_2O_3/MWCNT (red), and (b) CO/CH_4 yield profiles 1% Pd +2.3% La_2O_3/MWCNT.

programmed CO_2 reduction conditions the 1% Pd/MWCNT sample shows very low CO_2 conversion activity even at 500 °C. In contrast, the 0.5% Pd/Al_2O_3 (in which the Pd particle size is comparable to this catalyst) displays very high activity under the same reaction conditions, as we have shown in Figure 1. Interestingly, completely different CO_2 reduction activity pattern was measured over the La_2O_3-containing Pd/MWCNT sample: the CO_2 conversion level was comparable to that of the 0.5% Pd/Al_2O_3 catalyst. These results strongly suggest that single Pd atoms without the presence of an oxide in their immediate vicinity are unable to catalyze the reduction of CO_2 with H_2. This also brings up a very interesting point about the role of the alumina support in this catalytic system: it can not only be considered as a mere support for the active metal phase but also as an active component in this complex catalytic system. In the Pd+La_2O_3/MWCNT system the lantana promoter plays the same role as alumina in the Pd/Al_2O_3 catalysts. In both systems the oxides (La_2O_3 promoter and Al_2O_3 support) are completely inert in the reduction of CO_2, although they interact with CO_2 rather strongly. However, for the reduction of CO_2 to proceed, both CO_2 and H_2 need to be activated. This can only be done on bi- or multifunctional catalysts. The oxides in question here (La_2O_3 and Al_2O_3) are not able to activate (dissociate) H_2. For this functionality a metallic component needs to be present in the catalyst (here Pd).

On the basis of this hypothesis, we now can rationalize our observations on the CO_2 reduction activities of our supported Pd catalysts. In the 1% Pd/MWCNT catalyst, Pd (present in atomic dispersion) can activate H_2, but the functionality to activate CO_2 is absent. Therefore, this material is inactive in the reduction of CO_2 with H_2 (Scheme 1, reaction (I)). In the

Scheme 1

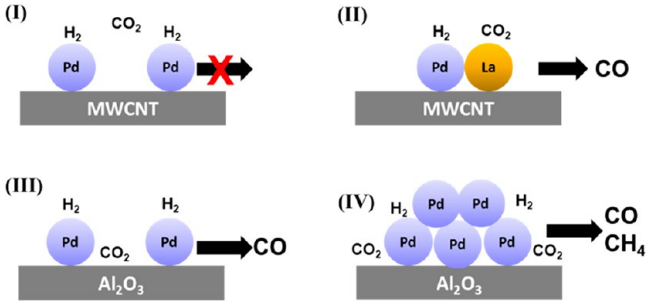

other two systems that also contain Pd in atomic dispersion but in the presence of oxide components (0.5% Pd/Al_2O_3 and 1% Pd+2.3% La_2O_3/MWCNT) the reduction of CO_2 proceeds at high rates. This is due, most probably, to the concerted reaction between the oxide-activated CO_2 and the metal-activated hydrogen (Scheme 1, reactions (II) and (III)). But the reduction of CO_2 in these two systems produces primarily (or almost exclusively) CO, and not CH_4. This is the consequence of the absence of Pd metal clusters where the initially formed CO could be activated. The CO that forms from the oxide-activated CO_2 desorbs from these catalysts and is detected in the effluent. However, when Pd clusters are present in the system (10% Pd/Al_2O_3) the initially formed CO can readily be hydrogenated to CH_4 on the metal particles (both adsorbed CO and atomic hydrogen present on the metal clusters) (Scheme 1, reaction (IV)).[22] Therefore, the methane selectivity over the catalyst that contains large metal clusters is high. (Note that the methane selectivity also increases over the 0.5% Pd/Al_2O_3 catalyst at high temperatures due, most probably, to the sintering of the active Pd metal phase.)

Although the results presented in this study clearly show the effects of both metal particle size and the role of oxide support in the activation and reduction of CO_2, they do not allow us to propose a clear mechanistic picture. The mechanism of CO_2 reduction, specifically the formation of CH_4, on oxide-supported metal catalysts has been hotly debated in the literature, and no clear consensus had been reached.[23,24] Today

dx.doi.org/10.1021/cs4001392 | ACS Catal. 2013, 3, 2094−2100

it is generally accepted that CO_{ad} is the key intermediate in the CO_2 methanation reaction, and this CO_{ad} species is subsequently hydrogenated via the mechanism suggested for CO methanation.[25−27]. However, the mechanism of CO_{ad} formation itself is not without ambiguity. According to one proposal, CO_2 reduction produces CO_{ad} via the reverse water gas shift reaction through a formate intermediate.[26] Others have suggested a dissociative CO_2 adsorption as the source of CO_{ad} (and O_{ad}) via a redox mechanism of active metal centers ($CO_2 + M^{2+} \rightarrow MO_x + CO$, $H_2 + MO_x \rightarrow M^{2+} + H_2O$) followed by reduction of CO_{ad} to CH_4.[24,27,28] The formation of CH_4 from CO_{ad} was proposed to proceed either by the initial C−O bond breaking or with association of hydrogen with CO_{ad} and subsequent CO bond breaking. In earlier studies, CO dissociation was suggested as the first step, leading to active (as well as inactive) carbon species, that was hydrogenated stepwise to CH, CH_2, CH_3, and finally CH_4.[29−31] In these studies, adsorbed CH_x ad-species were proposed as reaction intermediates. In a different concept, CO disproportionation ($2CO \rightarrow C + CO_2$) was proposed as the initial step, followed by hydrogenation of the thus formed carbon to CH_4.[32,33] More recent studies indicated that a formyl $(HCO)_{ad}$ species played an important role in the CO methanation reaction, followed by C−O bond breaking and further hydrogenation[25,34]. This species was also identified as an intermediate in the dominant reaction pathway in DFT studies.[35] In a very recent study Ussa Aldana et al. questioned the necessity of CO formation in the methanation of CO_2 over supported Ni catalysts.[36] The results of their in operando FTIR spectroscopy study seem to suggest that the oxide-bound CO_2 is hydrogenated stepwise to form bicarbonates, formates, methoxides, and finally methane. By varying the oxide support, that is, modifying the acidity/basicity of the support and therefore the strength of CO_2-support interaction, the methanation activity of the supported Ni catalysts changed dramatically. While the results presented in this work cannot provide conclusive evidence for either of these proposed mechanisms, it clearly substantiates the need of a bifunctional catalyst for the activation/reduction of CO_2 on supported metal catalysts. It also underlines the importance of the metal-oxide interface in the overall CO_2 reduction process, and provides support for the initial step of the CO_2 reduction process, the formation of adsorbed CO, as critical in the path to CH_4 formation. In the absence of metal particles that can adsorb CO no CH_4 formation is observed, and CO is produced exclusively.

Although the results presented here clearly demonstrate the unique catalytic properties of atomically dispersed metals on solid supports, and the need of bifunctionality in the activation of CO_2, there are a number of key issues that needed to be addressed to establish a viable mechanistic picture for this catalytic process. Our current work is focusing on two key areas: determine the oxidation state and coordination environment of the active metal under working conditions, and understand the elementary steps of these reactions by carrying out careful kinetic measurements under both transient and steady state conditions.

CONCLUSION

The results of this study clearly show that atomically dispersed supported metals can be catalytically active even in the demanding reaction of CO_2 reduction. Their activity and selectivity patterns, however, differ by a large extent from those of 3D metal particles. The results of CO_2 hydrogenation reaction on Pd/Al_2O_3 and Pd/MWCNT catalysts have unambiguously proven the need of two different functionalities in an active catalyst. The reduction of CO_2 requires the presence of a catalyst component that is able to activate CO_2 (here either the support oxide (Al_2O_3) itself, or an oxide promoter (here La_2O_3)), and a metallic component (here Pd) that is able to dissociate H_2. When both of these functionalities are present the CO and CH_4 selectivities seem to be determined by the sizes of the metal particles present. The results presented here open a fundamentally new approach to the development of supported metal catalysts with specific activity and selectivity patterns: building single metal sites surrounded by materials providing multifunctionalities. This bottom-up approach may results in the development of new heterogeneous catalysts with activitites and selectivities resembling those of homogeneous metal-centered catalysts.

AUTHOR INFORMATION

Corresponding Author

*E-mail: Kwak@pnnl.gov (J.H.K.), janos.szanyi@pnnl.gov (J.S.). Phone: (509)-371-6234 (J.H.K.), (509)-371-6524 (J.S.).

Present Address

[§]School of Nano-Bioscience & Chemical Engineering, UNIST, Ulsan 689-798, Korea.

Notes

The authors declare no competing financial interest.

ACKNOWLEDGMENTS

The catalyst preparation and catalytic measurements were supported by a Laboratory Directed Research and Development (LDRD) project, while the TEM work was supported by the Chemical Imaging Initiative at the Pacific Northwest National Laboratory (PNNL). PNNL is operated for the U.S. Department of Energy by Battelle Memorial Institute.

REFERENCES

(1) Haruta, M. *Catal. Today* **1997**, *36*, 153.
(2) Chen, M.; Goodman, D. W. *Science* **2004**, *306*, 252.
(3) Lei, Y.; Mehmood, F.; Lee, S.; Greeley, J.; Lee, B.; Seifert, S.; Winans, R. E.; Elam, J. W.; Meyer, R. J.; Redfern, P. C.; Teschner, D.; Schlögl, R.; Pellin, M. J.; Curtiss, L. A.; Vajda, S. *Science* **2010**, *328*, 224.
(4) Qiao, B.; Wang, A.; Yang, X.; Allard, L. F.; Jiang, Z.; Cui, Y.; Liu, J.; Li, J.; Zhang, T. *Nat. Chem.* **2011**, *3*, 634.
(5) Boffa, A.; Lin, C.; Bell, A. T.; Somorjai, G. A. *J. Catal.* **1994**, *149*, 149.
(6) Wambach, J.; Baiker, A.; Wokaun, A. *Phys. Chem. Chem. Phys.* **1999**, *1*, 5071.
(7) Sneeden, R. P. A. *J. Mol. Catal.* **1982**, *17*, 349.
(8) Clarke, D. B.; Bell, A. T. *J. Catal.* **1995**, *154*, 314.
(9) Clarke, D. B.; Suzuki, I.; Bell, A. T. *J. Catal.* **1993**, *142*, 27.
(10) Boffa, A. B.; Bell, A. T.; Somorjai, G. A. *J. Catal.* **1993**, *139*, 6027.
(11) Peterson, A. A.; Abild-Pedersen, F.; Studt, F.; Rossmeisl, J.; Norskov, J. K. *Energy Environ. Sci.* **2010**, *3*, 1311.
(12) Park, J. N.; MacFarland, E. W. *J. Catal.* **2009**, *266*, 92.
(13) Kwak, J. H.; Hu, J. Z.; Mei, D. H.; Yi, C. W.; Kim, D. H.; Peden, C. H. F.; Allard, L. F.; Szanyi, J. *Science* **2009**, *325*, 1670.
(14) Kwak, J. H.; Tonkyn, R.; Tran, D.; Mei, D. H.; Cho, S. J.; Kovarik, L.; Lee, J. H.; Peden, C. H. F.; Szanyi, J. *ACS Catal.* **2012**, *2*, 1432.
(15) Wang, X.; Gorte, R. J. *Appl. Catal., A* **2002**, *224*, 209.
(16) Bradford, J.; Vannice, M. A. *J. Catal.* **1999**, *183*, 69.
(17) Yamaguchi, A.; Iglesia, E. *J. Catal.* **2010**, *274*, 52.

(18) Mei, D. H.; Kwak, J. H.; Hu, J. Z.; Cho, S. J.; Szanyi, J.; Allard, L. F.; Peden, C. H. F. *J. Phys. Chem. Lett.* **2010**, *1*, 2688.
(19) Tasis, D.; Tagmatarchis, N.; Blanco, A.; Prato, M. *Chem. Rev.* **2006**, *106*, 1105.
(20) Sun, Y. P.; Fu, K. F.; Lin, Y.; Huang, W. J. *Acc. Chem. Res.* **2002**, *35*, 1096.
(21) Osorio, A. G.; Silveire, I. C. L.; Bueno, F. L.; Bergmann, C. P. *Appl. Surf. Sci.* **2008**, *255*, 2485.
(22) Mei, D. H.; Rousseau, R.; Kathmann, S. M.; Glezakou, V.-A.; Engelhard, M. H.; Jiang, W.; Wang, C.; Gerber, M. A.; White, J. F.; Stevens, D. J. *J. Catal.* **2010**, *271*, 325.
(23) Eckle, S.; Anfang, H.-G.; Behm, R. J. *J. Phys. Chem. C* **2011**, *115*, 1361.
(24) Wang, W.; Wang, S.; Ma, X.; Gong, J. *Chem. Soc. Rev.* **2011**, *40*, 3703.
(25) Fisher, I. A.; Bell, A. T. *J. Catal.* **1996**, *162*, 54.
(26) Prairie, M. R.; Renken, A.; Highfield, J. G.; Thampi, K. R.; Grätzel, M. *J. Catal.* **1991**, *129*, 130.
(27) Liotta, F. L.; Martin, G. A.; Deganello, G. *J. Catal.* **1996**, *164*, 322.
(28) Ernsta, K. H.; Campbell, C. T.; Moretti, G. *J. Catal.* **1992**, *134*, 66.
(29) Goodman, D. W.; Kelley, R. D.; Madey, T. E.; Yates, J. T. *J. Catal.* **1980**, *63*, 226.
(30) Bell, A. T. *Catal. Rev. Sci. Eng.* **1981**, *23*, 203.
(31) Gupta, N. M.; Londhe, V. P.; Kamble, V. S. *J. Catal.* **1997**, *169*, 423.
(32) Mills, G. A.; Steffgen, F. W. *Catal. Rev. Sci. Eng.* **1974**, *8*, 159.
(33) Nijs, H. H.; Jacobs, P. A. *J. Catal.* **1980**, *66*, 401.
(34) Andersson, M. P.; Abild-Pedersen, F.; Remediakis, I. N.; Bligaard, T.; Jones, G.; Engbæk, J.; Lytken, O.; Horch, S.; Nielsen, J. H.; Sehested, J.; Rostrup-Nielsen, J. R.; Nørskov, J. K.; Chorkendorff, I. *J. Catal.* **2008**, *255*, 6.
(35) Inderwildi, O.; Jenkins, J. S.; King, D. *Angew. Chem., Int. Ed.* **2008**, *47*, 5253.
(36) Ussa Aldana, P. A.; Ocampo, F.; Kolb, K.; Louis, B.; Thibault-Starzyk, F.; Daturi, M.; Bazin, P.; Thomas, S.; Roger, A. C. *Catal. Today* DOI: 10.1016/j.cattod.2013.02.019.